

Fractal analysis of martensite in an Fe–Ni alloy

B. SKROTZKI

Institut für Werkstoffe, Ruhr-Universität Bochum, Postfach 102 148, 4630 Bochum 1, FRG

In general, microstructures can be described by microstructural parameters such as grain size or particle spacing, e.g. an average value can be obtained by quantitative metallography. In some cases these methods of classical quantitative metallography fail. For example, martensitic microstructures may appear highly disordered at the transition to microstructural chaos. They cannot be described by any average crystal size or particle spacing. A new approach has been applied to characterize a martensitic microstructure of an Fe–Ni alloy by fractal analysis. This includes the amount of martensite as well as the size spectra of martensite crystals and the distribution of residual austenite. In addition, the interface length martensite/austenite and the interface density were determined.

Nomenclature

α		martensite	n	(l)	reduction in scale by one iteration
β		austenite	N	(l)	number of segments of the fractal motive
d		Euclidian dimension: 0, 1, 2, 3	ρ	(μm^{-1})	interface density martensite/austenite
D		fractal dimension	S	(μm)	distance between areas of retained austenite
f_α	(l)	volume fraction of martensite	\bar{S}	(μm)	average austenite grain diameter
$f_{\alpha,x}$	(l)	volume fraction of martensite transformed by one iteration	S_x	(μm)	average martensite crystal length for a generation x
f_β	(l)	volume fraction of austenite	T_0	($^\circ\text{C}$)	temperature of metastable thermodynamical equilibrium
$f_{\beta,0}$	(l)	initial volume fraction of austenite	T_x	($^\circ\text{C}$)	transformation temperature for a fragmentation x
$f_{\beta,x}$	(l)	volume fraction of retained austenite after x fragmentations	ΔT	($^\circ\text{C}$)	undercooling below T_0 ; $\Delta T = M_s - T_0$
ΔH_x	(J g^{-1})	transformation enthalpy for a generation x	x	(l)	number of self similar iterations; fragmentation, generation crystals
L_0	(μm)	$\approx 3 \bar{S}$; initial interface line length			
L_x	(μm)	interface line length after x fragmentations			
M_s	($^\circ\text{C}$)	martensite start temperature			
M_f	($^\circ\text{C}$)	martensite finish temperature			

1. Introduction

In general, microstructures can be described by microstructural parameters such as grain size or particle spacing. By means of quantitative metallography it is possible to obtain average values for these quantities. For microstructural elements the Euclidian geometrical dimension, d , is usually used (Table I).

Martensite belongs to microstructures at the transition to chaos. In this case the methods of classical quantitative metallography cannot be applied because it is impossible to obtain an average particle spacing for martensite crystals. For a better characterization and understanding of martensitic transformation, fractal analysis could be a helpful “non-classical” method.

First, Mandelbrot [1] worked on systematic description of chaotic phenomena. Later, Hornbogen applied fractal analysis in material science to disordered and rugged morphologies [2–4].

The Sierpinski-gasket (Fig. 1) provides an analogy for a geometrical treatment of stepwise transformation to martensite. The triangle in Fig. 1 shows a simple model for formation of martensite, α , in an austenite grain, β . With every fragmentation, x , the number of segments, N , increases, whereas the size of an element, n , decreases. In contrast to the Euclidian dimension, d , the fractal dimension, D , need not be an integer. D is defined as

$$D = \frac{\log N}{\log 1/n} \quad (1)$$

The transformation from austenite β to martensite α starts at the austenite grain boundaries (Fig. 2). The transformation begins at the martensite start temperature, M_s , and is completed at the martensite finish temperature, M_f . M_s is determined by the temperature of the metastable thermodynamic equilibrium, T_0 , and the necessary undercooling, ΔT , to nucleate the

TABLE I Euclidian dimension of microstructural elements

<i>d</i>	Element	Hardening mechanism
0	interstitial atom	solid solution hardening
1	dislocation	work hardening
2	grain boundary	fine grain hardening
3	dispersed particle	precipitation hardening

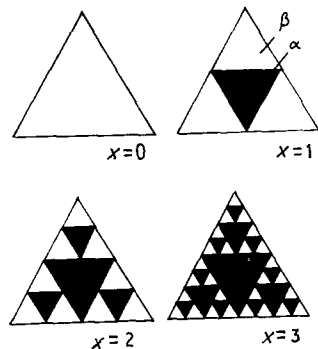


Figure 1 Sierpinski-gasket formed by subsequent fragmentations of a triangle; used as a model for martensitic transformation, α , in an austenite grain, β .

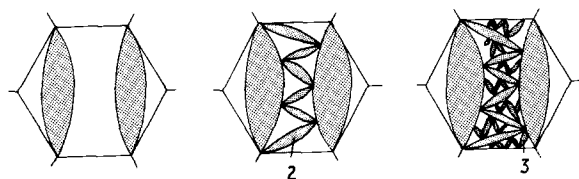


Figure 2 Subsequent formation of three generations of lenticular martensite crystals (schematic drawing) [4].

transformation

$$M_s = T_0 - \Delta T \quad (2)$$

In lenticular martensite a fractal microstructure forms, which can be characterized as: (i) more than $x \geq 3$ self similar fragmentations should be distinguishable (here generations of martensite crystals); (ii) a constant fractal dimension $D \neq d$ and self similarity should be observable for a range of more than one order of magnitude.

2. Experimental procedure

An iron-30.25 at % nickel alloy was melted as a 50 g button in an argon arc furnace using iron and nickel of electrolytic purity as starting material. The button was hot rolled (reduction in thickness of about 50%) and homogenized for 24 h at 1200 °C. An average grain size of $\bar{S} = 190 \mu\text{m}$ was established.

For differential scanning calorimetric (DSC) measurements, the "DuPont Thermal-analyser 9900" was used. The cooling rate amounts to 1°C min^{-1} .

The analysis of volume fraction martensite and austenite, respectively, and the determination of martensite/austenite interfaces were carried out with the "Quantimet 520" (Cambridge Instruments). In addition, the volume fraction of martensite was determined with calorimetric measurements.

3. Results and discussion

Fig. 3 shows a plot of the calorimetric measurements. The transformation from austenite to lenticular martensite proceeds stepwise in three generations. The transformation temperatures are indicated for every fragmentation. The transformed volume fraction can be calculated by dividing the enthalpy of each generation by the total enthalpy. The results are given in Table II. As the transformation is incomplete the total transformed volume fraction was determined by quantitative metallography to 73%. This quantity was considered in the calculations in Table II.

Fig. 4a shows the microstructure of the transformed DSC specimen. In accordance with the DSC measurements three generations of martensite crystals can be identified. Fig. 4b shows the microstructure of the same alloy after cold-rolling at $T = -196^\circ\text{C}$. It is closer to chaos than in Fig. 4a.

The self-similarity was tested by considering the ratio of length to thickness of the lenticular martensite particles. This ratio has to be constant. Subsequently, the average size and distribution function of different martensite generations were measured. The volume fraction as a function of number of fragmentations, x , is illustrated in Fig. 5.

At $T_1 = M_s$ the first generation $x = 1$ forms with an extension, S_1 , corresponding to the original austenite grain diameter. It transforms a volume fraction $0 < f_{\alpha,x=1} = 22.5\% < 1$. The second generation $x = 2$ can form at austenite/martensite interfaces at $T_2 < T_1$ with a spacing, S_2 , and a volume fraction $0 < f_{\alpha,x=2} = 39.9\% < 1$ in the untransformed spaces, etc. The number of possible fragmentations, x ,

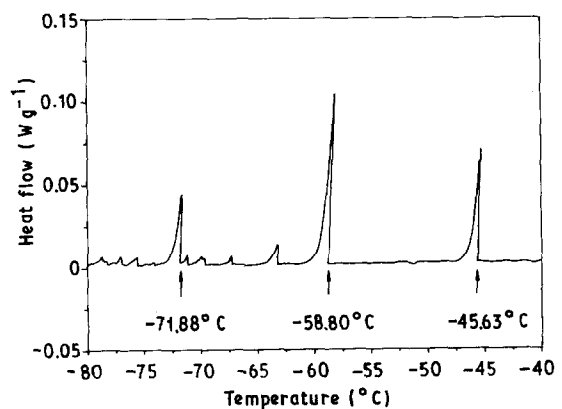


Figure 3 Heat flow and transformation enthalpy (see Table II) of Fe-30.25 at % Ni during the transformation from austenite to martensite. The transformation takes place in three sequential steps (transformation temperatures as indicated); mean cooling rate 1°C min^{-1} .

TABLE II Enthalpy of martensitic transformation and calculated volume fraction for different fragmentations

Fragmentation	T_x (°C)	ΔH_x (J g ⁻¹)	$f_{\alpha,x}$ (%)
$x = 1$	-45.63	1.734	16.75
$x = 2$	-58.80	3.408	32.92
$x = 3$	-71.88	2.415	23.33
Total	-	7.557	73.00

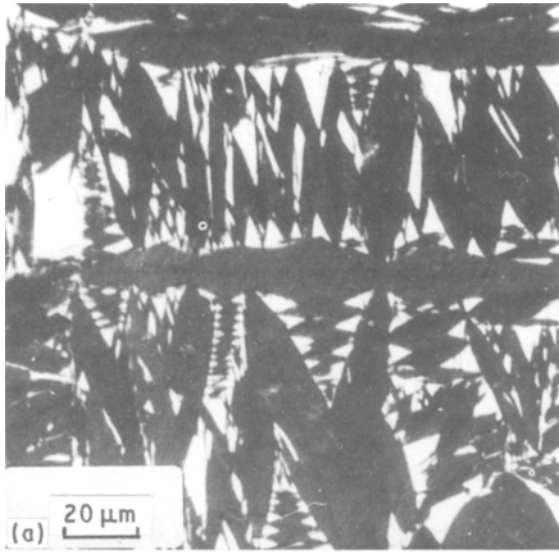


Figure 4 Microstructure of the transformed DSC specimen. (a) Undeformed, (b) cold-rolled at $T = -196\text{ }^{\circ}\text{C}$.

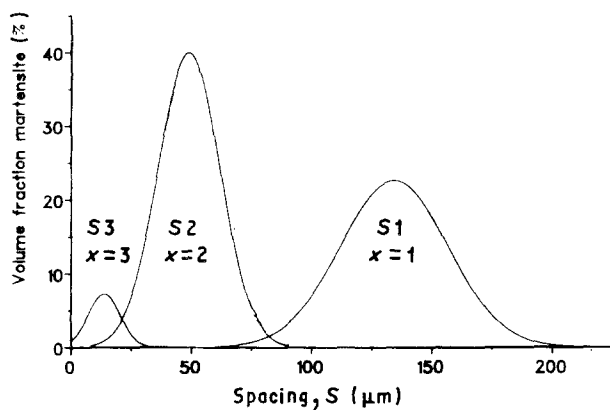


Figure 5 Volume fraction of martensite and size distribution as function of the number of fragmentations, x .

depends on the austenite grain diameter and on lateral growth of martensite. With increasing fragmentation further transformation becomes more and more difficult. Therefore, a large austenite grain size favours an increasing number of fragmentations.

It must be noticed that in the formation of the second generation the greatest volume fraction transforms. Normally it would be expected that the size of the transformed martensitic volume decreases with every fragmentation. In this case, it cannot be excluded that this result is a question of the selected picture detail because earlier measurements confirmed the expected decrease of the volume fraction with further transformation [5].

A fractal analysis of the residual austenite is also possible. The volume fraction, f_{β} , is given by $f_{\beta} = 1 - f_{\alpha}$. The spacing, S , is connected to the distance corresponding to neighbouring islands of different generations of residual austenite. The results are shown in Fig. 6. This figure also illustrates clearly that during the formation of the second generation the main volume fraction transforms.

It is evident from the model in Fig. 1 that the area and therefore the volume fraction, f_{β} , of the original triangle decreases in every fragmentation x by a factor of $\frac{3}{4}$

$$f_{\beta, x+1} = f_{\beta, x} (N/n) = f_{\beta, x} \left(\frac{3}{4}\right) \quad (3)$$

$$f_{\beta, x} = f_{\beta, 0} \left(\frac{3}{4}\right)^x \quad (4)$$

$$f_{\beta, x} = 1 - f_{\alpha, x} \quad (5)$$

$$f_{\beta, 0} = 1 \quad (6)$$

where $f_{\beta, 0}$ is the initial volume fraction of austenite.

The fractal dimension can be calculated using Equation 1. With $n = \frac{1}{4}$ (the size of α in the triangle) and $N = 3$ (number of segments β), the fractal dimension is $D \approx 0.792$. Fig. 7 shows the results. The volume fraction of retained austenite is plotted as a function of fragmentation x , temperature T and $(1/n)^x$.

The theoretical values from the Sierpinski-triangle are added to the results from the quantitative and calorimetric measurements. The quantities for the second and third generations are clearly below the theoretical values whereas the volume fraction of the first generation is slightly greater.

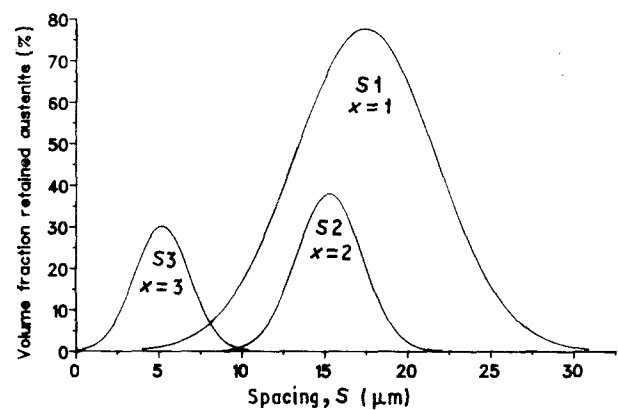


Figure 6 Variation of volume fraction and distribution of residual austenite with the number of fragmentations, x .

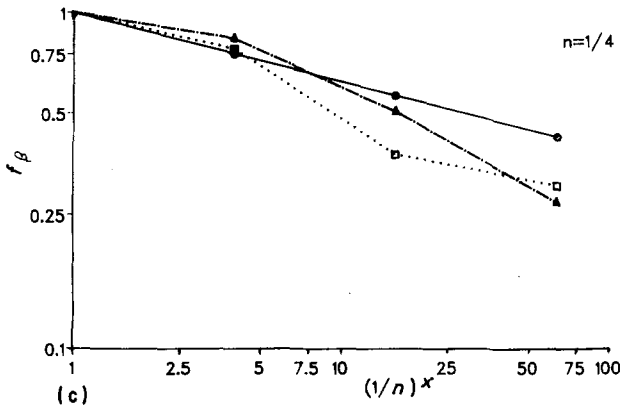
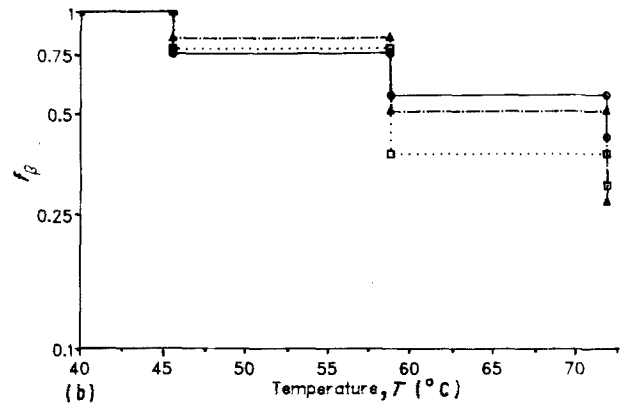
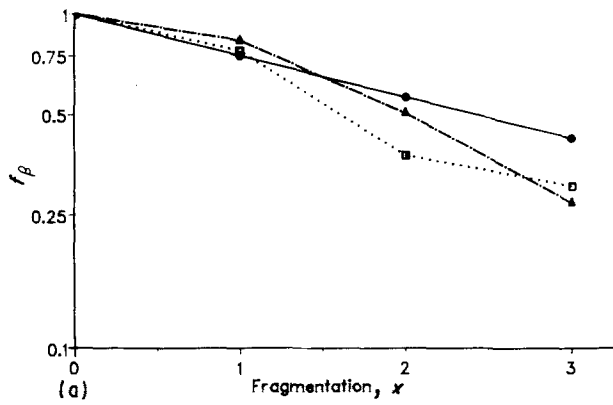


Figure 7 Decreasing volume fraction, f_{β} , of residual austenite during martensitic transformation with (a) the number of fragmentations, x ; (b) temperature, T , and (c) $(1/n)^x$ for $n = \frac{1}{4}$, according to (\cdots) quantitative and ($-\cdots-$) DSC measurements and ($---$) values for the Sierpinski-triangle.

new triangle is $n = \frac{1}{2}$ of the original triangle and the number of the created interface lines is $N = 3$. This provides a fractal dimension of $D = 1.585$ (Equation 1). The length of the interface, L_x , increases with every iteration

$$L_{x+1} = (Nn)L_x = \frac{3}{2}L_x \quad (7)$$

$$L_x = \left(\frac{3}{2}\right)^x L_0 \quad (8)$$

The length of the interface between austenite and martensite, L_x , depending on the number of fragmentations and temperature, was also measured. For the Sierpinski-gasket in Fig. 1 the line length of the

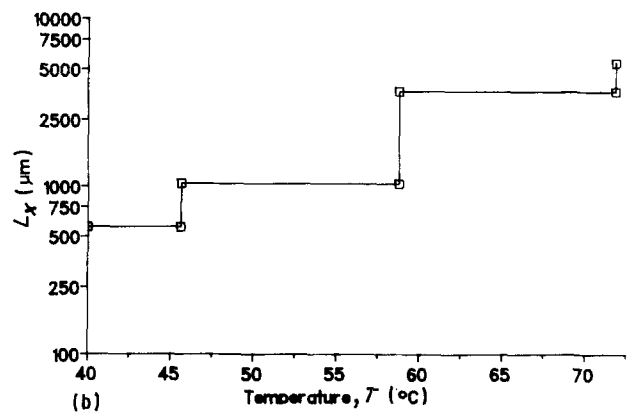
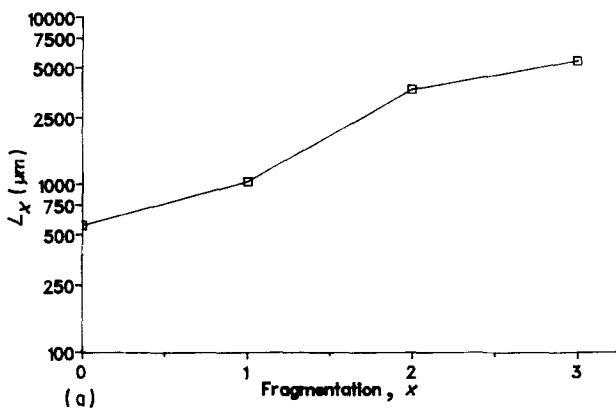


Figure 8 Increasing length of interface between martensite and austenite with (a) number of fragmentations, x and (b) temperature, T . (Quantimet.)

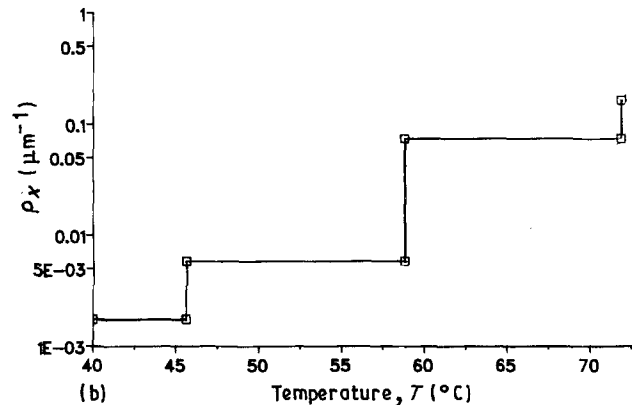
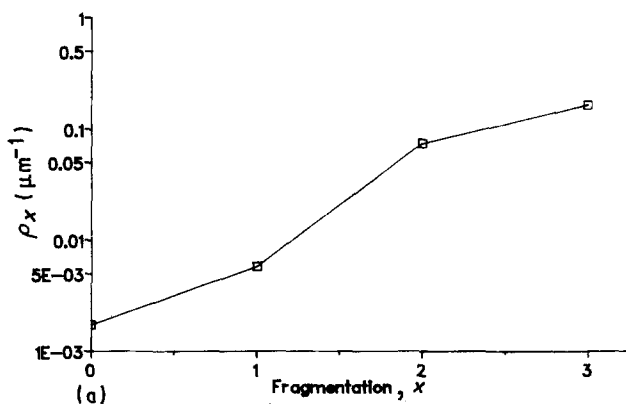


Figure 9 Increasing interface density as function of (a) number of fragmentations, x , and (b) temperature, T . (Quantimet.)

The initial line length was correlated to the average grain diameter, $L_0 \approx 3\bar{S}$ [3]. The results are illustrated in Fig. 8.

The interface density can be calculated from

$$\rho = \frac{\sum L_x^2}{L_0^3} \quad (9)$$

The calculations are represented in Fig. 9. The physical relevance of the model is not yet clear but the evidence of the fragmentation is indisputable (see Figs 3 and 4). If a quantitative description of fractal microstructures is possible, a derivation of relations between microstructures and properties should also be possible but this is an almost unexplored field. To provide evidence for this relation it is necessary to investigate a certain number of specimens.

Acknowledgement

This work was supported by the Stiftung Volkswagenwerk (I/63 844).

References

1. B. B. MANDELBROT, "The Fractal Geometry of Nature" (Freeman, New York, 1983).
2. E. HORNBOGEN, *Z. Metallkde* **78** (1987) 352.
3. *Idem, ibid.* **78** (1987) 622.
4. *idem, Int. Mater. Rev.* **34** (1989) 277.
5. B. SKROTZKI and E. HORNBOGEN, Proceedings of the International Conference on Martensitic Transformations, ICOMAT-89 (Trans Tech. Publications, 1990) p. 242.

*Received 22 February
and accepted 9 March 1990*